Equation of state of bismuth to 222 GPa and comparison of gold and platinum pressure scales to 145 GPa

Yuichi Akahama[a] and Haruki Kawamura
Faculty of Science, Himeji Institute of Technology, Koto, Kamogohri, Hyogo 678-1297, Japan

Anil K. Singh
Materials Science Division, National Aerospace Laboratories, Bangalore 560 017, India

(Received 2 April 2002; accepted 27 August 2002)

Unit cell volumes of Bi, Pt, and Au have been measured simultaneously to megabar pressures by x-ray powder diffraction using a diamond anvil cell and a synchrotron radiation source. The body-centered cubic (bcc) phase of Bi was found to be stable up to 222 GPa. The equation of state (EoS) of bcc-Bi was determined using the Pt pressure scale. A fit of the Vinet EoS to the volume compression data gave $B_0 = 35.22(19)$ GPa, $B_0' = 6.303(18)$, and 1 atm atomic volume $V_0 = 31.60(4)$ A^3. Because of the high compressibility, the use of bcc-Bi as a pressure marker is expected to give improved precision in pressure measurement. The Pt and Au pressure scales were compared up to 145 GPa. The Au pressure scale gave lower pressure than the Pt pressure scale. The deviation between the two scales became noticeable at ~30 GPa and diverged with increasing pressure, reaching ~20 GPa at 145 GPa. A fit of the Vinet EoS to Au compression data on the Ft pressure scale gave: $B_0 = 166.34(77)$ GPa, and $B_0' = 6.244(33)$. © 2002 *American Institute of Physics.* [DOI: 10.1063/1.1515378]

I. INTRODUCTION

In recent years powder x-ray diffraction experiments to 300 GPa have been successfully performed using a diamond anvil cell (DAC) and a third generation synchrotron as a source of the primary beam. In experiments at such high pressures, equations of state (EoS) of elemental metals are commonly used as pressure markers. The metals proposed for the pressure scale are Pt,[1,2] Au,[2–4] Ag,[5–7] Cu,[8] and Al.[8,9] In particular, the EoS of Pt has been well studied to 660 GPa with a two-stage gas gun and by a first-principle theoretical treatment.[1] These metals, except Al, have relatively low compressibility, limiting the precision of pressure determination. Further, the pressure scales provided by different materials remain to be compared.

Bismuth undergoes a number of pressure-induced structural phase transitions in a sequence: rhombohedral ($A7$)→ distorted simple cubic (dist. sc) →body-centered tetragonal (bct)→ body-centered cubic (bcc).[10–13] These transitions have been used as fixed points for pressure calibration at room temperature. In an earlier study[12] using the Au pressure scale,[2] the bcc Bi was found to be stable in the pressure range from 7.7 GPa to the highest pressure reached in the study (90 GPa) and much more compressible than Au and Pt. We show that bcc Bi is stable up to 222 GPa, the highest pressure reached in this study, and measure the EoS on the Pt pressure scale.[1] Because of its high compressibility, bcc Bi is a good choice for a pressure marker that will offer improved precision in pressure measurement. The bcc-Bi is found to be less compressible in the present study than in the earlier study,[12] wherein the pressure was estimated using the Au pressure scale.[2] By comparing the Pt and Au pressure scales, we show that this difference arises because the Au scale underestimates the pressure as compared to the Pt scale. The EoS of Au is measured on the Pt scale.

II. EXPERIMENTAL DETAILS

X-ray diffraction experiments were carried out at 300 K by an angle-dispersive method using an image plate (IP) detector and a primary beam of a wavelength 0.3292 A (or 0.3275 A) from the beam line BL04B2 at SPring-8.[14] The first set of experiments up to 145 GPa was performed with a 150 μm anvil face. The initial thickness of a precompressed Re gasket and the diameter of the central hole (sample chamber) were 24 and 65 μm, respectively. Samples of Bi (99,9999%), Pt (99.98%), and Au (99.98%) in form of thin foils of thickness 9, 7, and 7 μm, respectively, were stacked in the sample chamber. The shift of the fluorescence line from a micron-size ruby ball, also placed in the sample chamber, was used to monitor the sample pressure up to ~60 GPa. The pressure runs in these experiments will he referred to as Bi–Pt–Au runs hereinafter. The second set of experiments up to 222 GPa (referred to as Bi–Pt runs) was performed with a 50 μm anvil face. The initial thickness of a precompressed Re gasket and the diameter of the central hole (sample chamber) were 18 and 35 μm, respectively. The foil samples of Bi (I I μm) and Pt (7 μm) were stacked in the sample chamber. The incident beam was collimated to a 30 μm (or 26 μm) diameter. Typical exposure time was 15 min. The diffraction images were analyzed using the integration software PIP.[15] The x-ray wavelength, pixel size of the IP detector, and the sample-to-source distance were calibrated using the CeO_2 standard sample. The pressures values in this article are based on the EoS of Pt.[1]

[a]Author to whom correspondence should be addressed; electronic mail: akahama@sci.himeji-tech.ac.jp

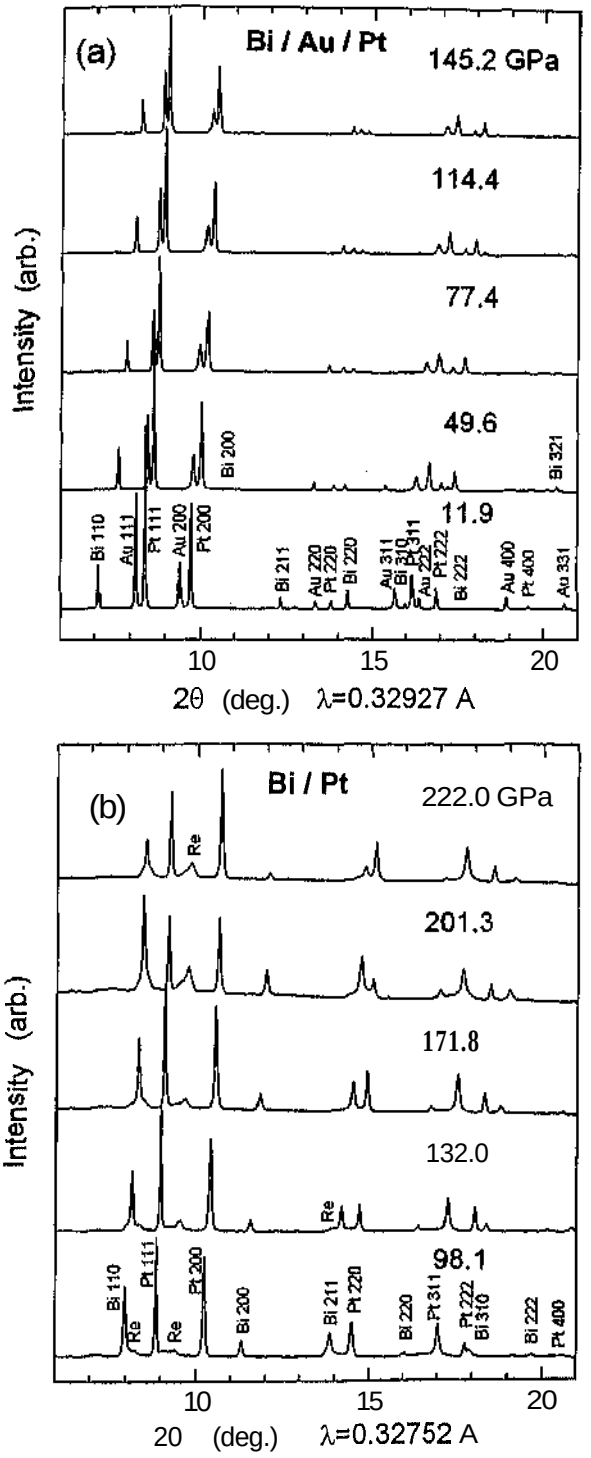

FIG. 1. Typical diffraction patterns at high pressures are from: (a) the Bi, Pt, and An samples in the first scries of experiments and (b) the Bi and Pt samples in the second series of experiments. Very low intensity of the (200) line from Bi in (a) was due to texturing of the sample.

III. RESULTS AND DISCUSSIONS

A. General

Figures 1(a) and 1(b) show typical diffraction patterns in two sets of experiments. The observed reflections were sharp without noticeable asymmetry and the number ranged between 4 and 6 for each sample. The lattice parameter $a_m(hkl)$ was calculated from each measured d spacing $d_m(hkl)$. The standard deviation in the lattice parameter

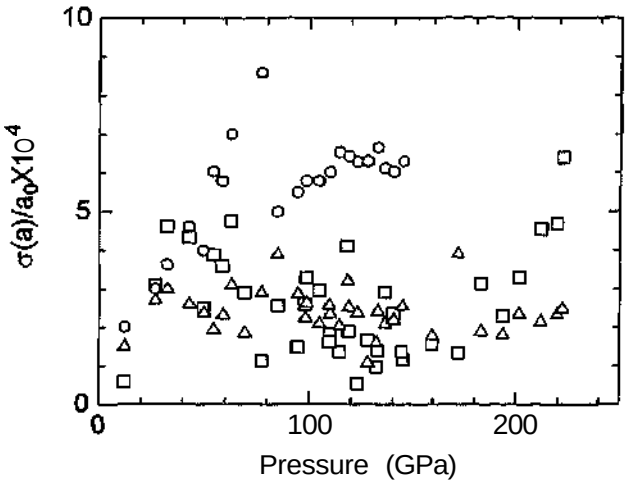

FIG. 2. Estimated standard deviations in the lattice parameters as a fraction of the one atmosphere lattice parameter versus pressure. The Bi, Pt, and Au data are shown by square, triangle, and circle respectively. Relatively large standard deviation in Au data arises from the presence of the nonhydrostatic compression effect.

$\sigma(a)$ calculated from $a_m(hkl)$ values for each run was small for Bi and Pt ranging between 0.0002 and 0.0015 (Fig. 2). Gold data showed a larger standard deviation that ranged from 0.0008 to 0.0028. The bcc Bi was found to be stable up to 222 GPa, the highest pressure reached in the present study. At 222 GPa, V/V_0=0.4735(10). This observation is consistent with the findings of a theoretical study" that predicted the stability of bcc Bi up to a compression of $V/V_0 \cong 0.4$.

B. Equation of state of bcc Bi

Figure 3 shows the measured atomic volumes of bcc Bi as a function of pressure on the Pt scale,[1] together with the data from an earlier study[12] conducted using the Mo $K\alpha$ radiation from a rotating-anode x-ray generator and the Au pressure scale.[2] The present data from Bi-Pt-Au and Bi-Pt

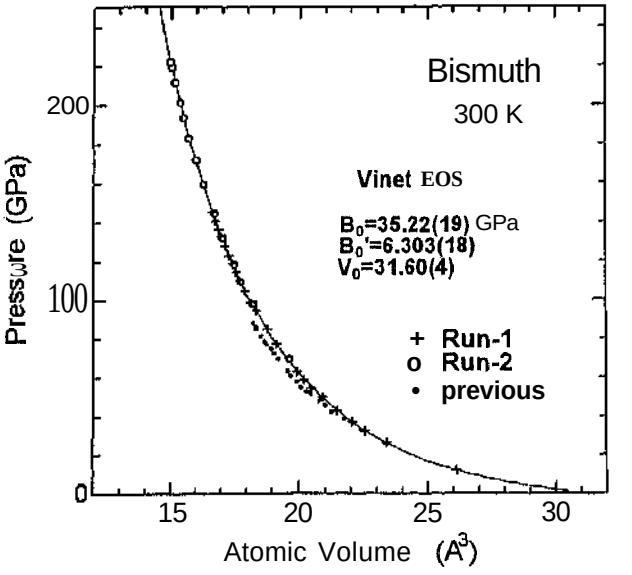

FIG. 3. Pressure dependence of atomic volume of bcc Bi. The solid line represents the least-squares fit of the Vinet equation to the present data. The error bar is within the size of the symbols.

TABLE I. Bulk modulus, pressure derivative of bulk modulus, and atomic volume at one atmosphere are listed.

	B_0 (GPa)	B_0'	V_0 (Å^3)	Equation	rms res.	P_{max} (GPa)	Reference
Pt	270	5.3	15.0946(48)	BM	—	91	2
	266	5.81		Vinet	—	660	1
Au	172	5.0	16.9671(66)	BM	—	83	2
	166.66	5.482		BM	—	70	3
	166.65	5.4S23		BM	—	216	4
	166.34(77)	6.244(33)		Vinet	0.2862	145	this article
	169.4(10)	5.94(5)		BM	0.3439	145	this article
Bi	35.22(19)	6.303(18)	31.60(4)	Vinet	0.4468	222	this article
	54.74(29)	4.905(19)	30.20(5)	BM	0.4818	222	this article

runs fall on a single curve. The compressibility of bcc Bi in the earlier study[12] is significantly higher than the compressibility in this study. As discussed in Sec. III C, this discrepancy arises because of a significant difference that exists between the Pt and Au pressure scales. The compression parameters for bcc Bi were derived by fitting standard equations of state (Vinet[17] and Birch-Murnaghan[18]) to the volume compression data. The atomic volume V_0 of bcc Bi at 1 atm was fixed by the following procedure. An extension of the compression data to $P=0$ graphically suggested that V_0 $=31$ Å^3. With this value of V_0, (V/V_0) versus P data were calculated and the Vinet EoS was fitted using nonlinear least squares and Marquardt–Levenberg algorithm treating B_0 and B_0' as the adjustable parameters. The calculations were repeated by varying V_0 in small steps around this value. Fit with $V_0=31.60(4)$ Å^3 gave the lowest root-mean-square (rms) of residuals. The results of fitting the Vinet and Birch-Murnaghan equations to the compression data are summarized in Table I. As judged from the rms of residuals, the Vinet equation was found to fit the compression data marginally better than the Birch equation. The uncertainty in (V/V_0) arises from the uncertainty in fixing V_0 and error in the measurement of V introduces.

C. Comparison of Au and Pt pressure scales

For a comparison of the Pt and Au pressure scales, we plot in Fig. 4 the pressures calculated from volume compression data of Au using the Jamieson's scale[2] and the Anderson scale[4] against the pressure obtained from the volume compression of Pt using the Holmes' scale.[1] The pressures estimated from the Jamieson's Pt scale are also given for comparison. The $x=y$ line helps in visualizing the deviation of the various pressure scales from the Pt scale.[1] The pressure obtained from the Jamieson's Pt scale is $\sim 3\%$ smaller than the pressure from the Holmes's scale in the entire pressure range. The discrepancy between the Jamieson's Au scale and the Holmes' Pt scale becomes noticeable at ~ 30 GPa and increases with increasing pressure reaching ~ 20 GPa at 150 GPa. The Anderson's Au scale shows a marginally better agreement with the Holmes' Pt scale. The pressures estimated from the ruby-line shift[18] below ~ 60 GPa lie between the Pt scale[1] and the Au scale.[2] The results of fitting the Vinet and Birch–Murnaghan (BM) equations to the volume compression data of Au on the Pt pressure scale[1] are shown in Table I.

A comparison of the Pt and Au scales based on data in Fig. 4 depends on the assumptions that the samples of different materials placed together in a DAC experience equal pressures. Further, the pressure on the sample has been assumed to be hydrostatic while the pressure is known to nonhydrostatic at such high pressures. The influence of these assumptions on the comparison of the Pt and Au scales is considered in Sec. III D It may be noted that the comparison between two Pt scales[1,2] (or two Au scales[2,4]) is independent of the present experimental data.

D. Analysis of stress state

The stress state of the sample compressed in a DAC is generally nonhydrostatic. The stress state at the center of the sample possesses an axial symmetry and is described by the axial (σ_3) and radial (σ_1) components.[19] The equivalent hydrostatic pressure is given by

$$\sigma_P=(\sigma_3+2\sigma_1)/3. \quad \text{(D}$$

Criterion for yielding of the sample material under compression suggests the following relation:

$$t=(\sigma_3-\sigma_1)\leqslant\sigma_Y=2\tau, \quad (2)$$

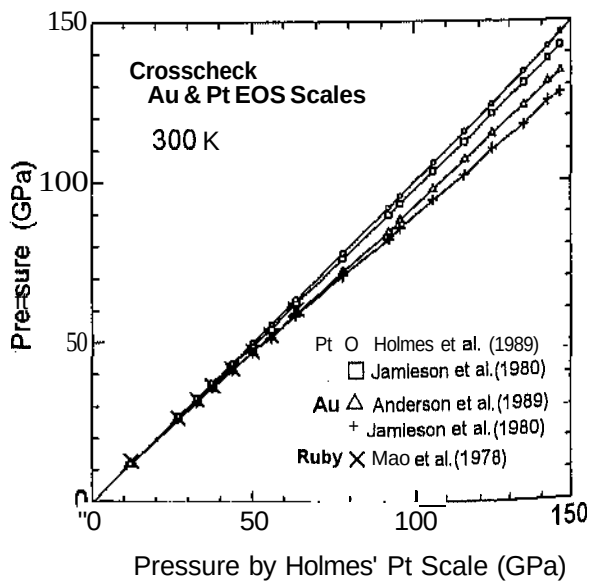

FIG. 4. A comparison of different pressure scales. The error bar is of the size of the symbols.

where σ_Y *is* the yield stress and r the shear strength of the sample material at σ_P. Equations (1) and (2) give

$$\sigma_P = \sigma_3 - 2t/3. \tag{3}$$

Consider the compression of a mixture of the sample and the pressure marker. Quite generally, the sample and the pressure marker develop stress states in accordance with Eqs. (1) and (2) with appropriate values of *t.* Some assumption connecting the stress states in the two has to be made to derive the sample pressure from the pressure computed using the measured volume compression and the EoS of the marker. Assumption that the marker and the sample experience equal pressures (continuity of pressure) is most likely to be valid when the experiments are done on intimate mixture of the sample and the marker, both in powder form. In the present experiments, the sample and the marker are in the form of foils. This configuration favors the continuity of σ_3 across the crystallites of the sample and the marker. Equation (3) suggests the following relation between the pressures in the sample and the marker:

$$\sigma_P(s) = \sigma_P(m) + 2[t(m) - t(s)]/3. \tag{4}$$

The second term on the right-hand side of Eq. (4) gives the difference between the sample pressures calculated assuming the σ_3 continuity and the σ_P continuity.

We now examine the effect of the nonhydrostatic stress on the volume compression data. The measured rf-spacing under nonhydrostatic compression is given by[19,20]

$$d_m(hkl) = d_P(hkl)[1 + (1 - 3\cos^2\psi)Q(hkl)], \tag{5}$$

where $d_P(hkl)$ is the d spacing under σ_P, ψ is the angle between the diffracting plane normal and the load axis of DAC, and $Q(hkl)$ is a term containing the single-crystal elastic compliances and t. For the cubic system[19,20]

$$Q(hkl) = (at/3)\{[2G_R^X(hkl)]^{-1} - (1 - \alpha^{-1})(2G_V)^{-1}\}, \tag{6}$$

where

$$[2G_R^X(hkl)]^{-1} = [S_{11} - S_{12} - 3S\Gamma(hkl)], \tag{7}$$

$$S = S_{11} - S_{12} - S_{44}/2, \tag{8}$$

$$\Gamma(hkl) = (h^2k^2 + k^2l^2 + l^2h^2)/(h^2 + k^2 + l^2)^2, \tag{9}$$

and

$$(2G_V)^{-1} = 5(S_{11} - S_{12})S_{44}/2[3(S_{11} - S_{12}) + S_{44}]. \tag{10}$$

The term a lies between 0 and 1. Recently it was shown[21] that for the cubic system $a_m(hkl)$ versus $3(1 - 3\cos^2\psi)\Gamma(hkl)$ plot (gamma plot) for the data recorded under the conventional DAC geometry can be approximated very closely to a straight line with a slope and an intercept, respectively,

$$M_1 = -a_P(atS/3), \tag{11}$$

and

$$M_0 = a_P\{1 + (at/3)(1 - 3\cos^2\psi) \times [(S_{11} - S_{12}) - (1 - \alpha^{-1})(2G_V)^{-1}]\}. \tag{12}$$

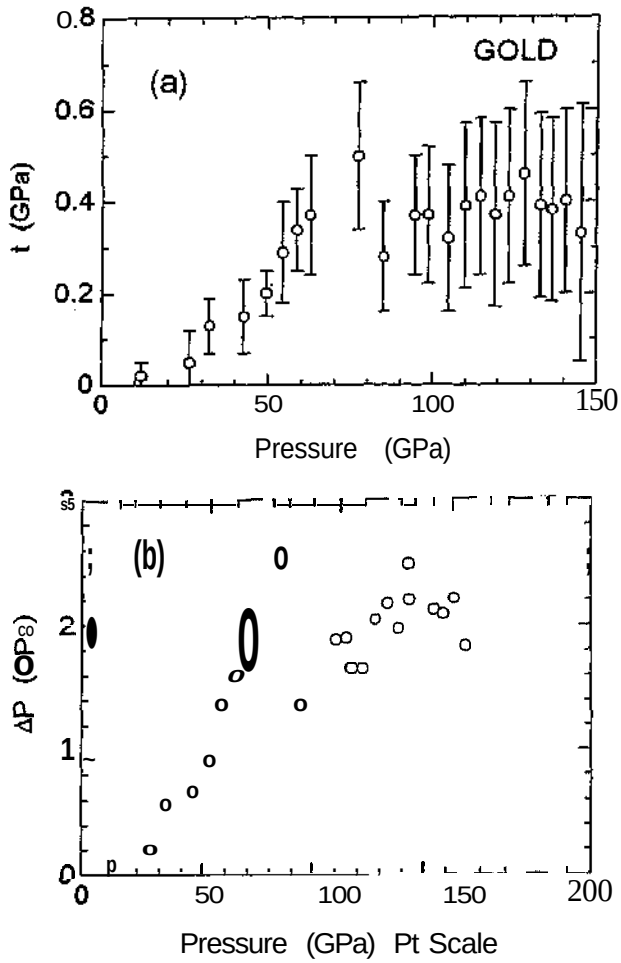

FIG. 5. Nonhydrostatic compression effect in Au data: (a) uniaxial stress components t as a function of pressure, and (b) error in pressure caused by the neglect of the nonhydrostatic compression effect at different pressures.

A very good estimate of (atS) can be made from such plots by using the relation

$$atS \approx -3M_1/M_0. \tag{13}$$

In the following discussion we use $\alpha = 1$. This choice for α gives the lowest estimate of the nonhydrostatic compression effect. The neglect of the nonhydrostatic compression effect results in an underestimation of the volume strain by

$$\Delta\epsilon_m(V) \approx 3\langle(1 - 3\cos^2\psi)Q(hkl)\rangle \times (a_P/a_0)^3, \tag{14}$$

where { } denotes the average value for all the observed reflections. The gamma plots for the Au data showed a good straight-line trend and *St* values were determined using Eq. (13). The S values at high pressure were estimated using Birch equations[22] and the single-crystal elasticity data.[23] The t values obtained from these data are shown in Fig. (5a). These values are in good agreement with the t values observed in earlier studies discussed elsewhere.[24] A fair degree of correlation is found between f and $\sigma(a)$. This is expected as the neglect of the nonhydrostatic compression effect[21] contributes to $\sigma(a)$. On correcting $a_m(hkl)$ for the nonhydrostatic compression effect using the procedure suggested

earlier,[21] $\sigma(a)$ reduces considerably. The volume strain is underestimated by an amount given by Eq. (14). The data in Figs. 5(a) and 5(b) suggest that $t = 0.40 \pm 0.06$ GPa and $\Delta P = 2.0 \pm 0.3$ GPa at 150 GPa. Extrapolations of these data using a logarithmic equation suggest that $t = 0.5 \pm 0.07$ GPa and the resulting $\Delta P = 2.7 \pm 0.3$ GPa at 222 GPa. A linear extrapolation of the data above 50 GPa gives practically the same result.

The gamma plots for Pt data from the Bi-Pt-Au set of experiments did not show straight-line trends ($R^2 \leq 0.4$). Such a situation can arise if the slope of the line is small in comparison with the standard deviation in the lattice parameter. The lack of the straight-line trend in the gamma plot does not always imply the hydrostatic stress state in the sample. A small (zero) slope indicates nearly hydrostatic (hydrostatic) pressure only if t is small (zero). The stress state may be significantly nonhydrostatic if a small (zero) slope arises from a small (zero) S. The estimate of t can be made in such a case by making use of the fact that t scales with the shear modulus[25] of the sample material. The 1 atm shear modulus of Pt is 63 GPa in comparison with 28 GPa for Au. Ignoring the influence on t of the presence of Au and Bi in the cell, t for Pt is expected to be ~ 2.2 times larger than the value for Au. Since $5 = 0.00388\ (\mathrm{GPa})^{-1}$ for Pt as compared with a value of $S = 0.02204\ (\mathrm{GPa})^{-1}$ for Au, St and therefore the slope of the gamma plot for Pt is expected to be smaller than the slopes of the gamma plots for Au by a factor of ~ 2.5. The estimated error in the volume strain of Pt is nearly half the value for Au. Considering the lower compressibility of Pt, the resulting error in pressure turns out to be approximately same as in case of Au. It is difficult to extend this discussion at high pressures, as the pressure derivatives of elastic constants for Pt are not available in the literature. The Pt data in 9 out of 14 runs from the Bi-Pt set of the experiments gave gamma plots showing reasonable straight-line trends with the sign of the slope predicted by Eq. (11) with 1 atm S_{ij} values. This indicates that 5 remains positive up to 222 GPa. The t values could not be calculated, as the information on pressure derivatives of single-crystal elastic constants for Pt is lacking. A measurement on Pt to ~ 20 GPa under nonhydrostatic compression has been attempted[26] recently using a radial diffraction geometry and the t and S values derived. The extrapolation of the t versus P data in the range $\sim 5-20$ GPa using a logarithmic equation suggests that $t = 8 \pm 2$ GPa at 150 GPa. In view of the large scatter inherent in such measurements and the wide range of extrapolation, the uncertainty in extrapolated value of t may be larger than indicated.

The use of a logarithmic equation for extrapolation of the low-pressure data to higher pressure has no real justification. However, this equation is used in the present work for the following reasons. The extrapolation of the data in Fig. 5(a) to 222 GPa is over a small range. As a result, the extrapolated value does not differ appreciably if a linear extrapolation is used or even if t above 5 GPa is assumed to be independent of pressure. However, the extrapolation of t versus P data on Pt[26] to 150 GPa does depend critically on the type of P-t relation used. The use of the linear extrapolation, for example, gives $t = 18 \pm 6$ GPa at 150 GPa, with marginally poorer fit than the logarithmic equation. This value of t appears to be very high considering the fact that Pt is a bcc metal. The t versus P data obtained from high-pressure diffraction experiments often exhibit a steep initial rise and a flattening at higher pressures. Such behavior is interpreted in terms of two straight lines that indicate two distinct deformation processes. It is the flattening of the curve at high pressures that is simulated very well by a logarithmic equation. This feature of the logarithmic fit is amply demonstrated by the fact the extrapolated value of t for Pt changes from 8 GPa at 100 GPa to 8.7 GPa at 200 GPa.

The gamma plots with Bi data, for both Bi-Pt-Au and Bi-Pt series of experiments, do not exhibit straight-line trends. However, the Bi data in 9 out of 14 runs from the Bi-Pt set of experiments gave gamma plots showing reasonable straight-line trends. These are the same runs wherein the Pt data gave good gamma plots. The sign of the slopes in these plots suggests that S is positive for bcc Bi. A detailed analysis of the bcc Bi data is not possible as the elastic moduli and the pressure derivatives of bcc Bi are not known. An extrapolation using the Birch equation[22] suggests that, at any pressure below 250 GPa, the bulk modulus of bcc Bi remains less than the bulk modulus of Au. Assuming, though not justifiably, that the Poisson's ratios for bcc Bi and Au are equal, the shear modulus of bcc Bi at any pressure below 250 GPa is expected to be less than that of Au. This would suggest that the magnitude of t in bcc Bi is not very different from that in Au.

E. Systematic errors in pressure

The two factors discussed in the preceding section introduce systematic errors in the pressure estimation. The neglect of the nonhydrostatic compression effect results in an underestimation of pressure. A limited analysis suggests that the magnitude of error in all the samples is nearly equal and increases with increasing pressure, reaching ~ 3 GPa at 150 GPa. Thus, σ_P is $\sim 2\%$ larger than the pressure calculated from the measured volume strain and the EoS. The correction for the nonhydrostatic effect does not alter Fig. 4 significantly which is constructed assuming the pressure continuity between Pt and Au samples. On the other hand, if the continuity of σ_3 is assumed then Eq. 4 suggests that the y coordinate of the Au datum at $x = 150$ GPa in Fig. 4 will increase by ~ 5 GPa and y coordinates of other points will increase proportionately. This will bring the line for Au closer to the $x = y$ line but not enough to bring about a good agreement between the Pt^1 and Au^2 scales. A good agreement between the two scales requires an increase of ~ 20 GPa in the y coordinate at $x = 150$ GPa. Therefore, the conclusions of Sec. III C in this article are not effected by these uncertainties.

F. Random errors in pressure

In the Bi-Pt-Au runs the highest pressure as determined from the volume compression of Pt was 145.2 ± 0.8 and 145.50 ± 0.22 GPa from the bcc Bi compression data. The errors indicated correspond to $\sigma(a)$. The highest pressure in the Bi-Pt runs was estimated to be 222.0 ± 1.0 GPa from

both Pt and bcc Bi compression data. The advantage of higher compressibility of bcc Bi is annulled by larger $\sigma(a)$ observed in the highest-pressure range (Fig. 2). The high degree of precision in pressure estimation is also indicated by low rms of residuals in the EoS fit to bcc Bi compression data. For the reasons discussed earlier in this article, the pressures in the Bi–Pt–Au runs estimated from compression data of Au using the Jamieson's pressure scale are consistently lower than the corresponding values estimated from Pt data. The highest pressure is estimated to be 128.9± 1.5 GPa. Large error in pressure arises from large $\sigma(a)$, a consequence of neglecting the nonhydrostatic compression effect in case of the systems exhibiting large elastic anisotropy.[21]

IV. SUMMARY

The bcc Bi is stable up to the highest pressure (222 GPa) reached in this study. Because of its high compressibility, bcc Bi promises to offer high precision in pressure measurement, the uncertainty introduced by the errors in volume–compression measurements being 0.1% at low pressure and 0.5% at the highest pressure. The Au pressure scale[2] systematically underestimates pressure in comparison with the Pt pressure scale.[1] Because of similar considerations the Pt pressure scale[1] has been preferred in a recent study on the EoS of stishovite.[27] The EoS of Au has been reported on the Pt pressure scale.[1]

ACKNOWLEDGMENTS

The authors thank K. Kondo, T. Yagi and K. Takemura for helpful discussions and Y. Ohishi for his help in diffraction experiments at SPring-8 conducted under Proposal No. 2000B0178-CD-np. The work was supported by Japan Society for Promotion of Science (Grant No. 12640321) and Ministry of Education, Science, Sports and Culture (Grant No. 12126204). Thanks are due to the referee for comments and making available preliminary data on Pt. A.K.S. acknowledges support under CSIR emeritus scientist scheme and thanks Denis Andrault for making available the preprint of his article.

[1] N. C. Holmes, J. A. Moriarty, G. R. Gathers, and W. J. Nellis, J. Appl. Phys. 66, 2962 (1989).
[2] J. C. Jamieson, J. N. Fritz, and M. H. Manghanani, Adv. Earth Planet. Sci. 12, 27 (1980).
[3] D. L. Heinz and R. Jeanloz, J. Appl. Phys. 55, 885 (1984).
[4] O. L. Anderson, D. J. Isaak, and Y. Yamamoto, J. Appl. Phys. *65*, 1534 (1989).
[5] W. J. Carter, S. P. Marsh, J. N. Fritz, and R. G. McQueen, in *Accurate Characterization of the High Pressure Environment*, edited by E. C. Lloyd (U. S. Washington DC, 1971), pp. 189-200.
[6] K. Syassen and W. B. Holzapfel, J. Appl. Phys. 49, 4427 (1978).
[7] J. Xie, S. P. Chen, S. Gironcoll, and S. Baroni, Philos. Mag. B 79, 911 (1999).
[8] W. J. Nellis, J. A. Moriarty, A. C. Mitchell, M. Ross, R. G. Dandrea, N. W. Ashcroft, N. C. Holmes, and G. R. Gathers, Phys. Rev. Lett. *60*, 1414 (1988).
[9] R. G. Greene, H. L. Luo, and A. L. Ruoff, Phys. Rev. Lett. 73, 2075 (1994).
[10] H. Iwasaki and T. Kikegawa, Acta Crystallogr., Sect. B: Slruct. Sci. **B53**, 353 (1997).
[11] K. Aoki, S. Fujiwara, and M. Kusakabe, J. Phys. Soc. Jpn. **51**, 3826 (1982).
[12] Y. Akahama, M. Kobayashi, and H. Kawamura, *Proceeding of 31st High Pressure Conference of Japan*, Osaka, Japan, 1990, pp. 392-393.
[13] M. I. McMahon, O. Degtyareva, and R. J. Nelmes, Phys. Rev. Lett. **85**, 4S96 (2000).
[14] *SPring-8 Beamline Handbook 2001* (Japan Synchrotron Radiation Research, Hyogo, 2001), p. 20.
[15] O Shimomura, K. Takemura, H. Fujihisha, Y. Fujii, Y. Ohishi, T. Kikegawa, Y. Amemiya, and T. Matsushita, Rev. Sci. Instrum. 63, 967 (1992).
[16] P. Vinet, J. Ferrante, J. H. Rose, and J. R. Smith, J. Geophys. Res. 92, 9319 (1987).
[17] F. Birch, Phys. Rev. 71, 809 (1947).
[18] H. K. Mao, P. M. Bell, J. W. Shaner, and D. J. Steinberg, J. Appl. Phys. 46, 3276 (1978).
[19] A. *K.* Singh, J. Appl. Phys. 73, 4278 (1993); 74, 5920 (1993).
[20] A. K. Singh, C. Balasingh, H. K. Mao, R. J. Hemley, and J. Shu, J. Appl. Phys. **83**, 7567 (1998).
[21] A. K. Singh and K. Takemura, J. Appl. Phys. 90, 3269 (2001).
[22] F. Birch, J. Geophys. Res. 83, 1257 (1978).
[23] B. Golding, S. C. Moss, and B. L, Averbach, Phys. Rev. 158, 637 (1967).
[24] T. S. Duffy, G. Shen, D. L. Heinz, J. Shu, Y. Ma, H. K. Mao, R. J. Hemley, and A. K. Singh, Phys. Rev. B 60, 15 063 (1999).
[25] J. 0. Chua and A. L. Ruoff, J. Appl. Phys. 46, 4659 (1975).
[26] A. Kavner and T. S. Duffy (private communication)
[27] D. Andrault, R. J. Angel, J. N. Mosenfelder, and T. Le Bihan, Am. Mineral. (communicated),